Chemical short-range order in amorphous Ni-Ti alloys: an integral equation approach with a non-additive hard-sphere model

1989 J. Phys.: Condens. Matter 1 3469

(http://iopscience.iop.org/0953-8984/1/22/008)

J. Phys.: Condens. Matter **1** (1989) 3469–3487. Printed in the UK

Chemical short-range order in amorphous Ni–Ti alloys: an integral equation approach with a non-additive hard-sphere model

D Gazzillo†, G Pastore‡ and S Enzo†

† Dipartimento di Chimica Fisica, Universita' di Venezia, S. Marta 2137, 30123 Venezia, Italy

‡ International School of Advanced Studies, Strada Costiera 11, 34014 Trieste, Italy

Received 19 July 1988, in final form 14 November 1988

Abstract. We analyse some of the most recent experimental scattering data for amorphous Ni–Ti alloys in terms of a non-additive hard-sphere (NAHS) model.

The relevant correlation functions and structure factors are obtained by solving numerically the Ornstein–Zernike integral equations, supplemented by the Percus–Yevick closure, for Ni_x–Ti_{1-x} systems with $x = 0.3$, 0.4, 0.5 and 0.7. A comparison between additive and non-additive hard-sphere models is presented for $x = 0.5$. Satisfactory semi-quantitative agreement with experimental data is then found for the $Ni_{40}Ti_{60}$ glass.

The model is able to account for the appearance of a prepeak in the diffraction pattern as a natural consequence of the set-up of a chemical short-range order (CSRO) in the system. The usefulness of non-additive hard-sphere models for describing CSRO in metallic glasses is carefully discussed.

1. Introduction

It is well known that in most of the liquid and amorphous multi-component materials the atomic distribution around the atoms of each species differs from the average one corresponding to a completely random mixing. In a random (ideal) mixture the local number density of i and j atoms around an i-type atom is the same as that around a j-type one. On the contrary, in real systems deviations from such an ideal behaviour may produce a tendency for like atoms to be neighbours (homo-coordination) or a preference for unlike neighbours and consequent compound formation (hetero-coordination). The correlation in space of the resulting composition fluctuations with respect to a random distribution is usually called 'chemical (or compositional) short-range order' (CSRO).

When such ordering phenomena are strong enough, all the measured structural and thermodynamic properties show marked deviations from ideality. In particular, in some (liquid and amorphous) binary metallic alloys experimental evidence for a preferred hetero-coordination is given by an unusual prepeak in the total structure factor $S^x(k)$ obtained by x-ray diffraction as a function of the wavevector k. The origin of this prepeak from compositional fluctuations can be demonstrated with the help of neutron scattering experiments. In fact, under particular conditions, these measurements allow the determination of the partial structure factor $S_{CC}(k)$ (Bhatia and Thornton 1970), which

0953-8984/89/223469 + 19 $02.50

contains information about concentration fluctuations of the two species: CSRO is then revealed by the presence of a pronounced $S_{CC}(k)$ peak at the same k-value of the prepeak observed with x-rays [this occurs, for example, in liquid Li–Pb (Ruppersberg and Hegger 1975) and amorphous Ni–Ti alloys (Ruppersberg *et al* 1980)].

From a theoretical point of view, the study of CSRO in compound-forming binary metallic alloys presents two distinct problems: (i) the choice of a good 'model', in the series of appropriate interaction potentials, and (ii) the calculation of the structural and thermodynamic properties from the assumed microscopic force laws.

Unfortunately, the true effective interatomic potentials of metallic systems have rather complicated forms with oscillatory (mainly attractive) tails (Hafner 1985). An accurate determination of these long-range contributions is required when *thermodynamic* quantities are to be evaluated (Hafner 1977, 1980, Pasturel *et al* 1985). On the contrary, if we are interested only in *structural* properties (partial pair distribution functions and static structure factors), suitably simplified potentials may be used, as a first good approximation. In many cases, for instance, hard-sphere (HS) potentials, soft inverse-power repulsions or hard-core interactions with screened Coulomb (Yukawa) tails yield physically sensible structural results. This follows from the fact that the structure of a condensed phase is dominated by the short-range repulsive forces (excluded volume effects), whereas the long-range interactions are rarely strong enough to induce *qualitative* changes of ordering (Hafner and Kahl, 1984, Kahl and Hafner 1985, Pasturel *et al* 1985).

In this paper we want to focus on the fact that the pair potentials of many binary alloys are *non-additive* (Kahl and Hafner 1985). This means that the distance between unlike nearest neighbours is not equal to the arithmetic mean of the distances between like components (i.e., $\sigma_{12} \neq (\sigma_{11} + \sigma_{22})/2$). Non-additivity may easily be observed from the partial radial distribution functions $g_{ij}(r)$ or from the position of the first peak in the partial structure factor $S_{12}(k)$, when it does not fall exactly midway between $S_{11}(k)$ and $S_{22}(k)$. In particular, for systems with strong hetero-coordinating tendency (such as, for instance, the above-mentioned liquid Li–Pb and amorphous Ni–Ti alloys), experimental data indicate a *reduction* in the distance between unlike nearest neighbours as compared with the average of the diameters of the pure metals.

With all this in mind, it becomes evident that the structural features of systems with strong CSRO cannot be modelled by HS mixtures with additive diameters R_{ij} [$R_{12} = (R_{11} + R_{22})/2$]. Therefore, to reproduce chemical ordering effects in liquid alloys, some authors (Copestake *et al* 1983, Hafner *et al* 1984, Pasturel *et al* 1985, Kahl and Hafner 1985, 1987) used potentials with both a repulsive short-range part and a long-range tail, chosen in such a way that the short-range terms are additive and non-additivity is generated by the long-range contributions. For instance, a simple model such as the symmetric HS–Yukawa (HSY) mixture (i.e., hard spheres of equal diameter plus repulsive Yukawa tails between like species and attractive ones between unlike species) can really yield a concentration–concentration structure factor $S_{CC}(k)$ with a marked peak.

In this context, the purpose of the present paper is to demonstrate that an HS model with *non-additive* diameters is already able to reproduce CSRO, i.e., the aforesaid behaviour of $S_{CC}(k)$, in amorphous binary alloys. Our aim is to investigate how CSRO and non-additivity are aspects related to the same physical reality and, with reference to amorphous Ni–Ti alloys, to show that the prepeak of $S^{x}(k)$ can be explained entirely in terms of excluded volume effects.

As concerns the choice of a statistical-mechanical route from the assumed interatomic potential to the determination of the structure, we then adopt an integral equation

method. To our knowledge, Weeks (1977) was the first to use the Percus–Yevick (PY) integral equation, well known in the theory of liquids (Boublik *et al* 1980), for studying the structure of metallic glasses by means of (additive) HS models. Clearly, the integral equations for liquid mixtures assume the presence of an homogeneous, isotropic phase and, consequently, they are unable to describe the crystalline state. Nevertheless, their results may be interesting for glassy systems. According to Weeks, the extension of these methods to the glassy state rests on the belief that the structural features of amorphous materials, especially those obtained by rapid quenching from the vapour or melt, are, in some sense, smooth extrapolations of those found in the stable fluid.

Unfortunately, from the analytic point of view, a complete solution of the PY integral equation for non-additive HS mixtures is still lacking; until now, only partial exact expressions, relevant to some particular cases, are available in the literature (Lebowitz and Zomick 1971, Perry and Silbert 1979, Gazzillo 1987, 1988). Therefore, in this work we have followed a completely numerical procedure for solving the Ornstein–Zernike integral equations within the PY approximation.

The paper is arranged as follows. In § 2 the non-additive HS model is presented and the basic formulae are recalled. Our numerical results, relevant to Ni–Ti alloys, are reported in § 3 and a comparison is made with both additive HS results and experimental data. Moreover, in § 4 we give a brief critical discussion on some aspects of our work and its relation to other possible approaches. Finally, the main results are summarised in § 5.

2. Model and formalism

2.1. Non-additive hard-sphere mixture and integral equations

Our model consists of a binary mixture of negatively non-additive hard spheres (NAHS). Defining R_{ij} to be the closest approach distance between the centres of two particles of species i and j (and $R_i \equiv R_{ii}$), the interaction potentials are given by

$$u_{ij}(r) = \begin{cases} +\infty & r < R_{ij} \\ 0 & r > R_{ij} \end{cases} \tag{1a}$$

with

$$R_{12} = \tfrac{1}{2}(R_1 + R_2)(1 + \Delta) \qquad \text{and} \qquad \Delta < 0. \tag{1b}$$

Note that $R_{12} < (R_1 + R_2)/2$, whereas in additive HS (AHS) mixtures ($\Delta = 0$) R_{12} is always equal to the arithmetic mean of the diameters R_1 and R_2 of the two species. In other words, negative non-additivity ($\Delta < 0$) simply means that a partial mutual penetration is allowed for *unlike* particles at contact.

Now, the knowledge of the equilibrium properties of this NAHS model requires the determination of the partial pair distribution functions (or partial radial distribution functions, RDF) $g_{ij}(r)$. To this aim, we solved numerically the Ornstein–Zernike (OZ) integral equations relating the direct correlation functions (DCF) $c_{ij}(r)$ to the total correlation functions $h_{ij}(r) \equiv g_{ij}(r) - 1$, i.e.,

$$h_{ij}(r) = c_{ij}(r) + \sum_k \rho_k \int \mathrm{d}\boldsymbol{r}'\, h_{ik}(|\boldsymbol{r} - \boldsymbol{r}'|)c_{kj}(r') \tag{2}$$

supplemented by the two closures

$$h_{ij}(r) = -1 \qquad r < R_{ij} \tag{3a}$$

$$c_{ij}(r) = 0 \qquad r > R_{ij}. \tag{3b}$$

Here ρ_k is the (mean) number density of the kth component (in the following, $\rho = \rho_1 + \rho_2$ will be the total number density and $x_i = \rho_i/\rho$ the concentration or atomic fraction of species i); moreover, equations (3*a*) and (3*b*), which are needed to complete the specification of the unknown functions, represent, for HS systems, the (exact) core condition and the Percus–Yevick (PY) approximation, respectively.

Note that, for a binary NAHS mixture, the OZ relations are a system of three coupled integral equations with five independent parameters: ρ_1, ρ_2, R_1, R_2 and R_{12} (or, equivalently, ρ, x_1, R_1, R_2 and Δ).

In the following, the component 1 will always be identified with Ni.

2.2. *Structure factors*

Let us now recall some basic definitions, which are quite general and independent of the HS model and PY approximation (Lele 1984, Waseda 1984).

The first quantity to be considered for a comparison between theory and experiment is the total x-ray structure factor defined by

$$S^x(k) = I^{\mathrm{coh}}(k)/I^{\mathrm{coh}}(k \to \infty) = \sum_{i,j} (x_i x_j)^{1/2} [f_i(k) f_j(k)/\langle f^2(k)\rangle] S_{ij}(k) \tag{4}$$

where $I^{\mathrm{coh}}(k)$ is the unnormalised coherent scattering intensity at a wavevector k, $f_i(k)$ is the atomic scattering factor for component i, $\langle f^2(k)\rangle = \Sigma_i x_i f_i^2(k)$ represents a compositional average and the $S_{ij}(k)$ are partial structure factors introduced by Ashcroft and Langreth (1967) (hereafter referred to as AL)

$$S_{ij}(k) = \delta_{ij} + (x_i x_j)^{1/2} \rho \hat{h}_{ij}(k) \tag{5}$$

(δ_{ij} is the Kronecker delta and $\hat{h}_{ij}(k)$ indicates the three-dimensional Fourier transform of $h_{ij}(r)$).

After solving the OZ integral equations for the DCFs $c_{ij}(r)$, the quantities $S_{ij}(k)$ are easily derived from the Fourier transforms $\hat{c}_{ij}(k)$ (Ashcroft and Langreth 1967).

However, in order to discuss the CSRO, it is convenient to take into account also an alternative decomposition of $S^x(k)$ in terms of partial structure factors proposed by Bhatia and Thornton (1970) (hereafter referred to as BT), i.e.,

$$S^x(k) = \frac{\langle f\rangle^2}{\langle f^2\rangle} S_{\mathrm{NN}}(k) + \frac{\langle f^2\rangle - \langle f\rangle^2}{\langle f^2\rangle} \frac{S_{\mathrm{CC}}(k)}{x_1 x_2} + 2\frac{\langle f\rangle \Delta f}{\langle f^2\rangle} S_{\mathrm{NC}}(k) \tag{6}$$

where $S_{\mathrm{NN}}(k)$, $S_{\mathrm{CC}}(k)$ and $S_{\mathrm{NC}}(k)$ are called the number–number, concentration–concentration and number–concentration structure factors, respectively; moreover, $\langle f\rangle = \Sigma_i x_i f_i$, $\Delta f = f_1 - f_2$ and $\langle f^2\rangle - \langle f\rangle^2 = x_1 x_2 (\Delta f)^2$ (remember that these quantities are k-dependent too).

Starting from the following linear combinations of pair distribution functions $g_{ij}(r)$ (Lele 1984),

$$g_{NN}(r) = x_1^2 g_{11}(r) + x_2^2 g_{22}(r) + 2x_1 x_2 g_{12}(r) \tag{7a}$$

$$g_{CC}(r) = x_1 x_2 [g_{11}(r) + g_{22}(r) - 2g_{12}(r)] \tag{7b}$$

$$g_{NC}(r) = x_1 x_2 [x_1 g_{11}(r) - x_2 g_{22}(r) + (x_2 - x_1) g_{12}(r)] \tag{7c}$$

the BT partial structure factors may be expressed as

$$S_{NN}(k) = 1 + \rho \hat{h}_{NN}(k) = x_1 S_{11}(k) + x_2 S_{22}(k) + 2(x_1 x_2)^{1/2} S_{12}(k) \tag{8a}$$

$$S_{CC}(k)/(x_1 x_2) = 1 + \rho \hat{g}_{CC}(k) = x_2 S_{11}(k) + x_1 S_{22}(k) - 2(x_1 x_2)^{1/2} S_{12}(k) \tag{8b}$$

$$S_{NC}(k) = \rho \hat{g}_{NC}(k) = x_1 x_2 [S_{11}(k) - S_{22}(k) + (x_2 - x_1) S_{12}(k)/(x_1 x_2)^{1/2}] \tag{8c}$$

(obviously, $h_{NN}(r) = g_{NN}(r) - 1$).

Equations (8) show the following short-wavelength behaviour: $S_{NN}(k \to \infty) = 1$, $S_{CC}(k \to \infty) = x_1 x_2$ and $S_{NC}(k \to \infty) = 0$. It is worth noting that for a random mixture it results that $S_{CC}(k) = x_1 x_2$ and $S_{NC}(k) = 0$ for all k values.

The functions $S_{NN}(k)$ and $g_{NN}(r)$ describe an 'average' atomic distribution irrespective of the species concerned (the so-called topological short-range order, TSRO).

On the other hand, CSRO can be investigated by studying the behaviour of the functions $g_{CC}(r)$ and $S_{CC}(k)$. In fact, from equation (7*b*) it follows that $g_{CC}(r)$ is negative at distances with predominant hetero-coordination, positive for preferred homo-coordination, and zero where the atomic distribution is locally random (evidently, it becomes zero also when all $g_{ij}(r)$ vanish inside the atomic cores). In Fourier reciprocal space, CSRO is then revealed, at some wavevector k, by strong deviations of $S_{CC}(k)$ from the value $x_1 x_2$ corresponding to randomness.

Finally, the cross terms $S_{NC}(k)$ and $g_{NC}(r)$ give information about concentration fluctuations induced by variations in the TSRO (and vice versa).

3. Numerical results and comparison with experimental data

Our theoretical analysis of the CSRO in Ni–Ti alloys may be divided conveniently into three parts. First, a comparison is made between the additive and non-additive HS model for $Ni_{50}Ti_{50}$, at different densities ranging from liquid-like to glassy-like values. Second, a NAHS mixture is used to fit experimental data of the amorphous $Ni_{40}Ti_{60}$ alloy and, in particular, to reproduce the prepeak in the total structure factor $S^x(k)$. Finally, varying x in Ni_xTi_{1-x} models, the dependence of the structural ordering on composition is also examined.

For *all* cases investigated, the PY integral equations were solved *numerically* by using Gillan's algorithm (Gillan 1979, Abernethy and Gillan 1980) with a grid of 512 points equally spaced ($\Delta r/R = 0.05$, where the unit of length R was chosen to be 1 Å).

In passing, we recall also that numerical solutions of the OZ integral equations for NAHS potentials have been published only for a relatively small number of cases, mainly concerning symmetric mixtures, i.e., binary systems with $R_1 = R_2$ and $x_1 = 0.5$ (Nixon and Silbert 1984, Ballone *et al* 1986, Gazzillo 1987, 1988). We are aware of results for only one asymmetric case with parameter values appropriate to compound-forming *liquid* alloys (Levesque *et al* 1980).

Note that, once the composition (i.e., the variable x_1) is fixed, the free parameters become four (ρ, R_1, R_{12}, R_2) in the NAHS model and three for an additive HS mixture.

First of all, the DCF $c_{ij}(r)$ and RDF $g_{ij}(r)$, together with the AL and BT partial structure factors, were evaluated. Then, calculating the atomic scattering factor for each species by means of an interpolation formula given by the *International Tables for X-ray Crystallography* (1969), the total structure factor $S^x(k)$ was determined according to equations (4) or (6).

Furthermore, we evaluated the coordination numbers and the generalised Warren CSRO parameter. Let us introduce the partial radial density function $\rho_{ij}(r) = x_j \rho g_{ij}(r)$, which represents the number of j-type atoms at a distance r from an i-type atom. The partial coordination number Z_{ij} is the number of j atoms in the first shell of an i-type atom and, for HS systems, it may be defined as

$$Z_{ij} = 4\pi \int_{R_{ij}}^{r_{ij}} r^2 \rho_{ij}(r)\, \mathrm{d}r \tag{9}$$

where r_{ij} is the position of the first minimum in $g_{ij}(r)$. Consequently, the total coordination number of species i, i.e., the total number of atoms in the first shell around an i-type atom, is approximately given by

$$Z_i = \sum_k Z_{ik}. \tag{10}$$

At this point, the generalised CSRO parameter α_w may be expressed as

$$\alpha_w = 1 - Z_{12}/(x_2 Z) = 1 - Z_{21}/(x_1 Z) \tag{11a}$$

with

$$Z = x_1 Z_2 + x_2 Z_1. \tag{11b}$$

The parameter α_w is a rough but useful measure of the CSRO: for a random distribution, α_w vanishes, while it becomes negative (positive) for systems with preferred nearest neighbour hetero- (homo-)coordination.

However, the numerical values of Z_{ij} and α_w must not be taken too literally. In fact, numerical uncertainty in α_w may be high, owing to some approximations contained in the previous relations. Moreover, we recall that some authors prefer a different method for counting the first neighbours, by using in equation (9), for all Z_{ij}, the same upper integration limit defined by the position of the first minimum in $g_{NN}(r)$. Clearly, the value of α_w depends on the definition adopted for Z_{ij}. Therefore, note also that a comparison with other published results makes sense only if Z_{ij} and the CSRO parameter are always determined in the same manner.

3.1. $Ni_{50}Ti_{50}$ alloy: a comparison between additive and non-additive HS models

In order to investigate whether a NAHS model may be able to reproduce the CSRO present in Ni–Ti alloys, we started with the case $x_1 = 0.5$. This is a convenient choice, since it avoids possible effects due to a difference in concentration of the two components. Moreover, the presence of CSRO in amorphous $Ni_{50}Ti_{50}$ is experimentally well established (Enzo *et al* 1988).

As concerns the geometrical parameters R_{ij}, R_1 and R_2 were assumed to be coincident with the nearest-neighbour distances of the crystalline pure components, i.e., $R_{Ni} = 2.49$ Å and $R_{Ti} = 2.89$ Å (Kittel 1976). Then, two alternative choices for R_{12} were considered, i.e., $R_{12} = 2.69$ Å ($\Delta = 0$, additive mixture) and $R_{12} = 2.56$ Å ($\Delta \simeq -0.048$), a value suggested by experimental data (Enzo *et al* 1988).

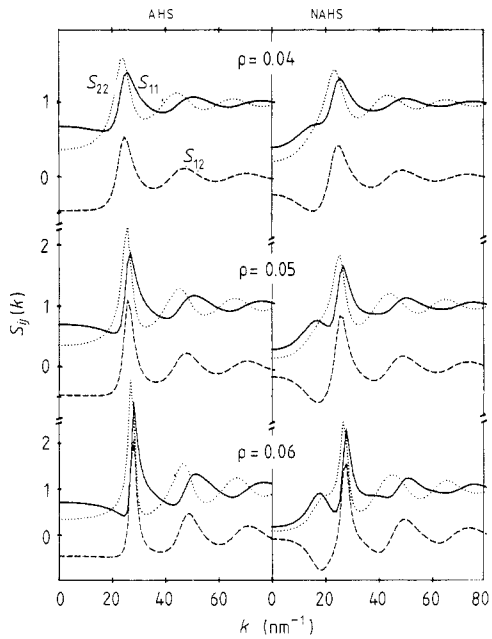

Figure 1. Comparison of Ashcroft–Langreth partial structure factors $S_{ij}(k)$ for $Ni_{50}Ti_{50}$ relevant to an additive hard sphere (AHS) model and a non-additive (NAHS) one with $R_{12} < (R_1 + R_2)/2$, at liquid-like and glass-like densities (left side ≡ figure 1(*a*); right side ≡ figure 1(*b*)). The parameter values are given in table 1. In all cases, the full, dashed and dotted lines represent $S_{11}(k)$, $S_{12}(k)$ and $S_{22}(k)$, respectively.

To reach the high values relevant to glassy states, the mean total density was varied stepwise starting from a very low initial point and, consequently, a sequence of results was generated. Clearly, this procedure allows to follow also the possible evolution of CSRO from the liquid to the amorphous state. In a sense, this part of our theoretical analysis is similar to some experimental studies performed to answer the question whether the CSRO originates in the glass-forming process itself or in the liquid state. We recall, for instance, the work by Sakata *et al* (1981): by neutron diffraction measurements on liquid and amorphous $Cu_{66}Ti_{34}$ alloys, these authors demonstrated that the CSRO is already present in the liquid phase and is enhanced on vitrification.

Our numerical results for the $S_{ij}(k)$ and BT partial structure factors are plotted in figures 1 and 2, respectively. Here, a comparison is made between additive and non-additive HS models at three different densities, i.e., $\rho = 0.04$, 0.05 and 0.06 atoms/Å^3 (in the following, dimensionless densities will be used, with ρ representing ρR^3).

For both models, as the density increases, the amplitude of the oscillations in $S_{ij}(k)$ becomes progressively larger, while the position of the first peak moves towards higher k values. The differences between additive and non-additive mixtures are, however, evident (compare figure 1*a* and *b*). Note that in the additive case, the AL partial structure factors retain essentially the same qualitative characteristics with increasing ρ. On the contrary, the corresponding functions of the NAHS system have a shape that exhibits a notable evolution and is very different from the additive one in the region to the left of the main peak. In particular, in $S_{11}(k)$ at $\rho = 0.04$ it is noteworthy the appearance of a shoulder, which becomes a true pre-peak in the interval $k \approx 1.7$–1.9 Å^{-1} when $\rho = 0.05$, 0.06. At the same time and nearly at the same position as the aforesaid pre-peak, a deep

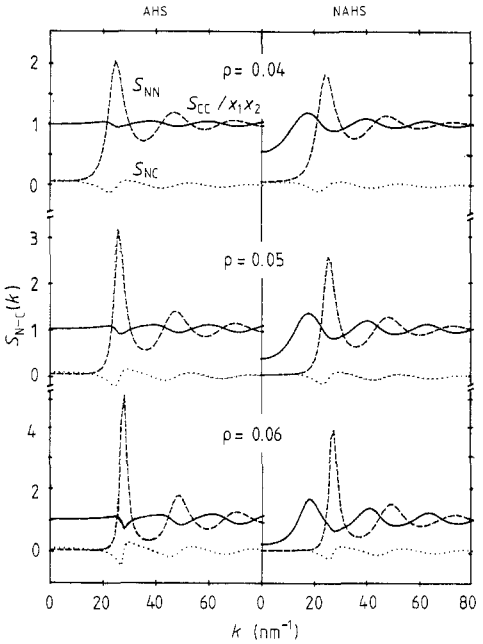

Figure 2. Comparison of Bhatia–Thornton partial structure factors $S_{N-C}(k)$ relevant to an additive (left side ≡ figure 2(*a*)) and a non-additive (right side ≡ figure 2(*b*)) HS model for $Ni_{50}Ti_{50}$, at liquid-like and glass-like densities. The parameter values are given in table 1. In all cases, the full, dashed and dotted lines represent $S_{CC}(k)/(x_1x_2)$, $S_{NN}(k)$ and $S_{NC}(k)$, respectively.

negative minimum and a shoulder arise in $S_{12}(k)$ and $S_{22}(k)$, respectively. According to equation (8*b*), which yields $S_{CC}(k)/(x_1x_2) = [S_{11}(k) + S_{22}(k) - 2S_{12}(k)]/2$ when $x_1 = 0.5$, this behaviour of the functions $S_{ij}(k)$ generates a well defined peak in $S_{CC}(k)/(x_1x_2)$ in the same region (figure 2*b*). The position of this peak in $S_{CC}(k)$ at a *smaller* k value than that corresponding to the first peak in $S_{NN}(k)$ may be explained as follows: in the alloy, in addition to the fundamental topological short-range order, there is a pseudo-periodicity A–B–A–B which is produced by the tendency for unlike atoms to be neighbours and involves a *longer* characteristic length than the topological first-neighbour distance (Sakata *et al* 1981).

These results show clearly that a NAHS model is able to exhibit concentration fluctuations *strongly deviating* from randomness, i.e., a true CSRO in liquid and amorphous $Ni_{50}Ti_{50}$ alloys. On the contrary, this effect is practically absent in the additive HS model (see figure 2(*a*) and compare also the values of the parameter α_w reported in table 1).

It is rather surprising to see how our naïve choice of non-additive diameters R_{ij} works well. However, it is not good enough to produce a true pre-peak in $S^x(k)$, at least at the above-mentioned density values. In the best non-additive case ($\rho = 0.06$) only a small shoulder was obtained. In fact, the weighting factor of $S_{CC}(k)/(x_1x_2)$ in equation (6) is proportional to the square of the difference in the atomic scattering factors of the components and is rather small for this alloy. However, we did not attempt to search for a better choice for the parameters (ρ, R_1, R_{12}, R_2). In fact, a fit to experimental data is not very convenient in the case of $Ni_{50}Ti_{50}$ glass, since only the total structure factor $S^x(k)$ is available (Enzo *et al* 1988).

Table 1. Density dependence of the partial coordination numbers Z_{ij} and generalised CSRO parameter αw for $Ni_{50}Ti_{50}$: comparison between additive and non-additive HS models. The closest approach distances R_{ij} and the density ρ are expressed in Å and in atoms/Å^3, respectively. The non-additivity parameter Δ and the packing fraction η are dimensionless.

R_1	R_{12}	R_2	R_1/R_2	R_{12}/R_2	Δ	ρ	η	Z_{11}	Z_{12}	Z_{22}	α_w
2.49	2.69	2.89	0.86	0.93	0	0.04	0.41	5.25	5.98	6.59	−0.004
						0.05	0.52	5.25	6.04	6.80	−0.001
						0.06	0.62	5.26	6.14	7.13	0.004
2.49	2.56	2.89	0.86	0.89	−0.048	0.04		4.87	6.18	6.54	−0.040
						0.05		4.86	6.38	6.54	−0.056
						0.06		4.37	6.72	6.63	−0.100

Finally, it is also interesting to note that, at each density value, the height of the main peak in $S_{ij}(k)$ and $S_{NN}(k)$ for the NAHS model is always smaller than that corresponding to the additive case. Presumably, this effect may be explained in terms of packing fraction η, defined as the ratio of the volume occupied by hard spheres to the total volume. In fact, it is easy to realise that, under the same values of the parameters ρ, R_1 and R_2, the model with negative non-additivity will always have a smaller packing fraction than the additive one, in consequence of the possible overlap of hard cores. We recall that for an additive HS mixture the packing fraction is simply given by $\eta = (\pi/6)\Sigma_i \rho_i R_i^3$. Unfortunately, in presence of non-additivity, the volume occupied by hard spheres becomes dependent on the microscopic atomic configuration and it is not possible to obtain a simple exact expression for η.

In passing, we recall that according to Cargill (1975) the packing fraction of most metallic glasses lies between 0.66 and 0.68 (note also that η is 0.74 for a FCC or HCP lattice and 0.68 for the BCC structure of single-component systems).

3.2. *$Ni_{40}Ti_{60}$ alloy: a comparison between the* NAHS *model and experimental data*

Although interpretation of results in r-space is more physically understandable, we preferred to fit experimental data for the $Ni_{40}Ti_{60}$ glass directly in reciprocal space. In fact, owing to the finite range of accessible k-values, Fourier transformation of experimental data may introduce undesired spurious effects.

The theoretical structure factors, obtained from our NAHS model within the PY approximation, were compared with the corresponding quantities measured and published by Ruppersberg *et al* (1980), Wagner and Lee (1980), Fukunaga *et al* (1984). As concerns the x-ray total structure factor $S^x(k)$, the data found in the first reference look more reliable in the region of the pre-peak in which we are interested. On the other hand, the third paper is of fundamental importance for us, since also the Bhatia–Thornton and Faber–Ziman partial structure factors are reported there (the Faber–Ziman functions can be converted easily into the AL ones).

Performing a fit without having at our disposal any analytic theoretical expression is not a simple task. We adopted a 'trial and error' procedure to fit, first of all, the main peaks of all structure factors, varying the four independent parameters ρ, R_1, R_{12}, R_2 around realistic values.

The total mean number density ρ was estimated by means of the approximate relation $\rho \approx x_{Ni}\rho_{Ni} + x_{Ti}\rho_{Ti}$, where ρ_{Ni} and ρ_{Ti} refer to the crystalline pure components. Since

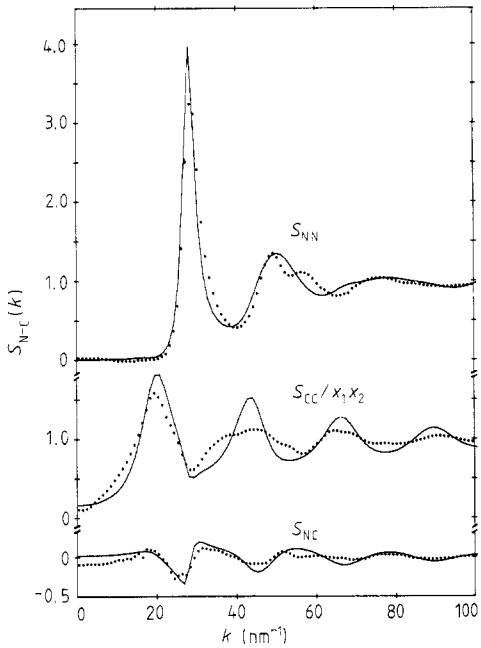

Figure 3. BT partial structure factors $S_{N-C}(k)$ for the $Ni_{40}Ti_{60}$ glass: the dots are experimental data by Fukunaga *et al* (1984) and the full curve represents the theoretical results obtained from the NAHS model with $(\rho, R_1, R_{12}, R_2) = (0.065, 2.40, 2.45, 2.85)$.

$\rho_{Ni} = 0.0914$ and $\rho_{Ti} = 0.0566$ (Kittel 1976), it results that $\rho \approx 0.07$ for the $Ni_{40}Ti_{60}$ alloy. Accordingly, we explored the density range 0.06–0.07, with steps $\Delta\rho = 0.001$.

As concerns the parameters R_{ij}, it is clear that there is no need to identify the *effective* HS diameters R_i with the nearest-neighbour distances in the crystalline pure species or with those measured in the alloy. Nevertheless, we hoped to get a fit by using R_{ij} values not too far from the experimental ones. Therefore, we allowed R_1, R_2 and R_{12} to be varied stepwise in the intervals (2.40, 2.60), (2.75, 3.00) and (2.40, 2.60) Å, respectively (usually with steps $\Delta R_{ij} = 0.05$ Å, but sometimes with $\Delta R_{ij} = 0.01$ Å).

Although more than 50 cases were analysed, it was not possible to achieve a complete disentanglement of the dependence of the structure factors on each of the parameters (ρ, R_1, R_{12}, R_2). Some qualitative trends are, however, worth reporting:

(i) At fixed R_{ij}, as the density increases, the position of the main peak in $S_{ij}(k)$ and, consequently, in $S_{NN}(k)$ and $S^x(k)$ shifts towards higher k values;

(ii) At a fixed ρ, the position of the main peak in $S_{ij}(k)$ is, to a first approximation, proportional to $1/R_{ij}$.

(iii) The height of the maxima of the structure factors mentioned in item (i) is an increasing function of both ρ and R_{ij}. Presumably, it is related to the total packing fraction η.

(iv) As already discussed in § 3.1, the features of $S_{CC}(k)/(x_1x_2)$, which reveal the presence of CSRO, are essentially determined by the values of the geometrical variables R_{ij}, i.e., by the ratios R_1/R_2 and R_{12}/R_2 (or, equivalently, R_{12}/R_1 and R_2/R_1). For a given set of parameters ρ, R_1 and R_2, the height of the first peak becomes larger with increasing non-additivity (i.e., with $|\Delta|$); at the same time, the maximum of $S_{NN}(k)$ decreases,

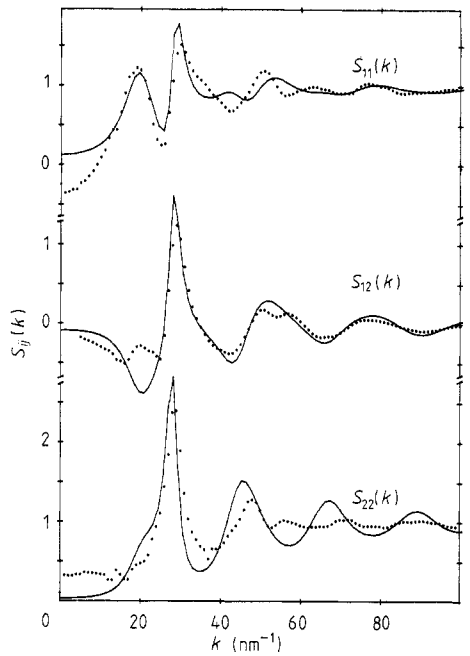

Figure 4. AL partial structure factors $S_{ij}(k)$ for the $Ni_{40}Ti_{60}$ glass: the dots are experimental data by Fukunaga *et al* (1984) (we have converted Faber–Ziman functions to AL ones) and the full curves represent the theoretical results obtained from the NAHS model with $(\rho, R_1, R_{12}, R_2) = (0.065, 2.40, 2.45, 2.85)$.

presumably as a consequence of the lowering of packing fraction. Moreover, at fixed R_{ij}, the peaks in $S_{CC}(k)/(x_1x_2)$ become more pronounced with increasing ρ.

We started from the choice $(\rho, R_1, R_{12}, R_2) = (0.06, 2.50, 2.55, 2.90)$, which coincides practically with the last case considered for the $Ni_{50}Ti_{50}$ alloy, but at a different composition. With respect to the experimental data, the resulting theoretical $S^x(k)$ exhibits a shift toward the origin and a less intense pre-peak. To correct these shortcomings, it was necessary to increase the density [item (i)] and, at the same time, we reduced suitably the values of all R_{ij} [item (ii)], mainly to avoid too large packing fractions and consequently too high main peaks in the structure factors [item (iii)].

One of our best sets of results corresponds to the choice $(\rho, R_1, R_{12}, R_2) = (0.065, 2.40, 2.45, 2.85)$. The relevant BT and AL partial structure factors, together with $S^x(k)$, are plotted in figures 3, 4 and 5, respectively. For a comparison with experiment, data by Fukunaga *et al* (1984) were used in the first two figures, but we preferred the $S^x(k)$ given by Ruppersberg *et al* (1980) for figure 5, since it exhibits a better definite pre-peak.

A good *overall* agreement between theory and experiment is evident, mainly in the region before and around the first peak of the structure factors. First of all, it is to be noted that the NAHS model is really able to exhibit a marked pre-peak in $S^x(k)$. In the inset of figure 5 we plot also an even better pre-peak, obtained with another good choice of parameters, i.e., $(\rho, R_1, R_{12}, R_2) = (0.065, 2.40, 2.50, 2.85)$. This shows how varying only R_{12}, in the direction of decreasing non-additivity, allows a further improvement in the shape of the pre-peak to be obtained. Moreover, with these new parameter values, the maximum of $S_{CC}(k)/(x_1x_2)$ is reduced and a better agreement with the corresponding

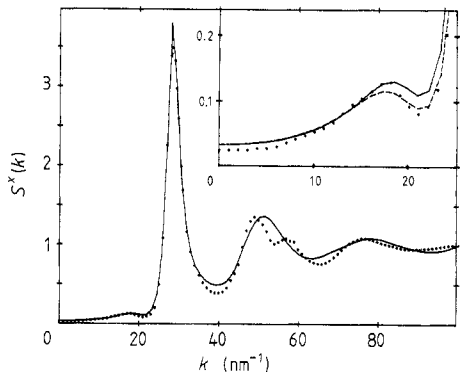

Figure 5. Total x-ray structure factor $S^x(k)$ for the $Ni_{40}Ti_{60}$ glass: the dots are experimental data by Ruppersberg *et al* (1980) and the full curve represents the theoretical results obtained from the NAHS model with $(\rho, R_1, R_{12}, R_2) = (0.065, 2.40, 2.45, 2.85)$. In the inset, the dashed curve corresponds to the NAHS results relevant to the choice $(\rho, R_1, R_{12}, R_2) = (0.065, 2.40, 2.50, 2.85)$.

experimental data is achieved. Unfortunately, at the same time, the first peak in $S_{NN}(k)$ becomes higher, according to item (iv), and the maximum of $S^x(k)$ passes from 3.8 to 4.4. In this case our BT structure factors are, in the region of their first peak, very similar to those obtained for the same alloy by Hafner and Pasturel (1985) through a more complex thermodynamic variational approach, based on a symmetric HSY reference system.

However, apart from the uncertainty of the fitting procedure for the HS diameters R_{ij}, a difference in the first peak height between experimental and theoretical $S_{NN}(k)$ and $S^x(k)$ may also be due to a combination of other causes: experimental normalisation corrections, resolution of the measurement apparatus and the fact that the PY approximation tends to overestimate the amplitude of the first peak in $S_{ij}(k)$.

At this point, to discuss the region beyond the first peak of the structure factors, let us start with some general observations. It is well known from numerical results and analytical calculations (Hansen and Schiff 1973, Greenwood 1980) that one can relate the asymptotic decay and the phases of the $S_{ij}(k)$ to the steepness of the potential: the steeper the repulsive interaction, the slower is the decay to their asymptotic limit. In addition, there will be a dephasing of the oscillations such that the peaks after the first will appear shifted toward larger k values, with increasing the repulsiveness of the potential. For a particular model, Copestake *et al* (1983) provided further evidence that using potentials with soft repulsive cores may produce weaker and broader maxima in all the structure factors and even rather flat regions in $S_{CC}(k)/(x_1x_2)$. Then it is rewarding to find that most of the discrepancies between our results and the experimental ones can be accounted almost completely in terms of these systematic trends.

The only difference that is not explained is in the second peak of $S_{NN}(k)$ and $S^x(k)$. In fact, the experimental pattern exhibits a second maximum that is clearly split into a strong subpeak and a weak one (at $k \approx 4.95$ Å^{-1} and $k \approx 5.70$ Å^{-1}, respectively, while the first maximum is located at $k \approx 2.90$ Å^{-1}). Unfortunately, we were not able to reproduce such a behaviour of $S^x(k)$ by means of the NAHS model, within reasonable variations of the HS diameters.

As concerns the partial RDFs, our theoretical results exhibit a second peak splitting only in $g_{22}(r)$ (with subpeaks at $r \approx 2R_{12}$ and $r \approx 2R_2$, respectively). However, some

Table 2. Amorphous $Ni_{40}Ti_{60}$: comparison of our best theoretical NAHS results for Z_{ij} and α_w with experimental data. (*a*), (*b*) and (*c*) refer, respectively, to the works by Fukunaga *et al* (1984), Ruppersberg *et al* (1980) and Wagner and Lee (1980). Rigorously, the experimental α_w taken from Ruppersberg *et al* corresponds to the Warren–Cowley CSRO parameter.

R_1	R_{12}	R_2	R_1/R_2	R_{12}/R_2	Δ	ρ	Z_{11}	Z_{12}	Z_{22}	α_w
2.40	2.45	2.85	0.84	0.86	−0.067	0.064	2.55	7.69	8.39	−0.110
						0.065	2.54	7.08	8.39	−0.072
						0.066	2.44	7.79	8.44	−0.120
2.40	2.50	2.85	0.84	0.88	−0.048	0.064	2.72	7.74	8.26	−0.108
						0.065	2.64	7.81	7.41	−0.150
						0.066	2.61	7.90	8.33	−0.121
experimental										
(*a*) 2.63	2.60	3.01	0.87	0.86	−0.078	0.070	2.27	7.91	8.05	
(*b*)	2.6									−0.1
(*c*) 2.5	2.58	2.92	0.86	0.88	−0.048					−0.21

interesting results in the k-space will be reported in § 3.3 and a detailed discussion of these problems will be given in § 4.

Finally, table 2 gives the values of the partial coordination numbers Z_{ij} and CSRO parameter α_w relevant to our best cases, together with the experimental ones.

3.3. *Composition dependence of the* CSRO

Amorphous Ni–Ti alloys have traditionally been synthesised by liquid quenching in the composition range 25–40 at.% Ni (Polk *et al* 1978). Neutron and/or x-ray scattering results for samples prepared by using this technique are available also in the case of $Ni_{35}Ti_{65}$ (Wagner *et al* 1981), $Ni_{26}Ti_{74}$ ('zero alloy') and $Ni_{33}Ti_{67}$ glasses (Fukunaga *et al* 1981). To date, however, some new experimental methods, such as vapour quenching (Moine *et al* 1985) and mechanical alloying (Schwarz *et al* 1985), allow the synthesis of amorphous Ni_xTi_{1-x} systems in a wider composition range, i.e., $0.3 \leqslant x \leqslant 0.7$.

Therefore, to study the composition dependence of the CSRO, the three cases $x_1 = 0.3$, 0.5 and 0.7 were analysed and compared. However, we did not attempt any fit to experimental data, but we tried to get only some qualitative prediction from the NAHS model.

For sake of simplicity, it was assumed that the diameters R_{ij} are independent of the composition and coincident with those obtained from the fit for the $Ni_{40}Ti_{60}$ glass, i.e., $(R_1, R_{12}, R_2) = (2.40, 2.45, 2.85)$ Å. As concerns the total number density ρ, we adopted the simple relationship $\rho \approx C[x_{Ni}\rho_{Ni} + (1 - x_{Ni})\rho_{Ti}]$, where C is a rescaling constant chosen in such a way to yield $\rho = 0.065$ when $x_{Ni} = 0.4$. Within this approximation, ρ increases linearly with Ni concentration and it comes out that $\rho \approx 0.062$, 0.068 and 0.75 for $x_{Ni} = 0.3$, 0.5 and 0.7, respectively.

The relevant results for the AL, BT and total structure factors are plotted in figures 6, 7 and 8, respectively, so there is no need for long comments. In figure 6 it is worth noting the considerable evolution in the shape of $S_{11}(k)$ and $S_{22}(k)$ as the composition is varied. In particular, with increasing Ni content, the intensity of the pre-peak in

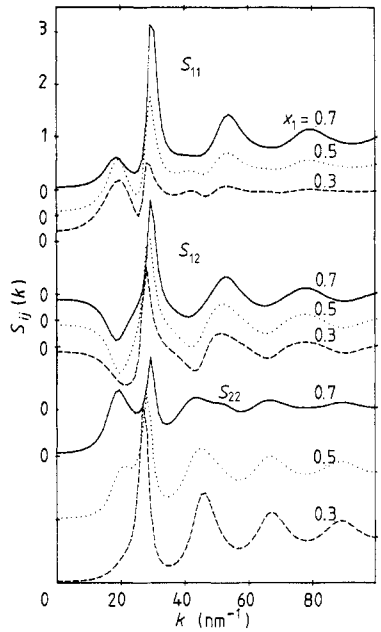

Figure 6. Concentration dependence of the AL partial structure factors $S_{ij}(k)$ relevant to a NAHS model for amorphous Ni_xTi_{1-x} alloys with $(R_1, R_{12}, R_2) = (2.40, 2.45, 2.85)$ Å. The density values, dependent on the Ni concentration x_1, are given in table 3.

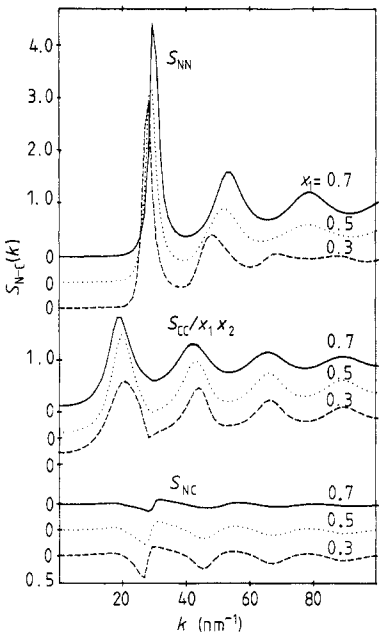

Figure 7. Same as in figure 6, but for the BT partial structure factors $S_{N-C}(k)$.

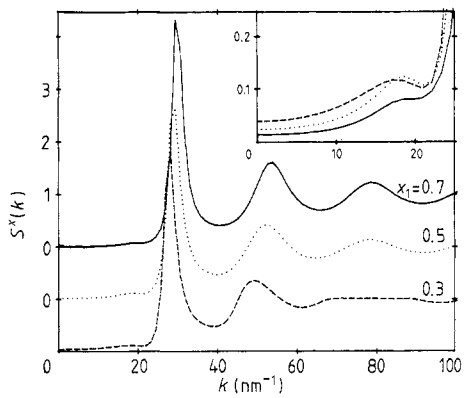

Figure 8. Same as in figure 6, but for the total x-ray structure factor $S^x(k)$.

$S_{11}(k)$ decreases, while a similar structure develops in $S_{22}(k)$. Moreover, special attention should be paid to a weak second peak splitting which occurs in $S_{22}(k)$ when $x_1 = 0.7$ and in $S_{11}(k)$ when $x_1 = 0.3$, respectively. This trend is a further element in favour of the NAHS model; even if the subpeaks or shoulders are located at incorrect positions, the existence of such splittings in the k-space, supports the opinion that the model may really be a first step in the right direction. For sake of completeness, it is to be noted also that in the r-space a clear second peak splitting is visible in $g_{22}(r)$ for

Table 3. Concentration dependence of the partial coordination numbers Z_{ij} and generalised CSRO parameter α_w, relevant to a NAHS model for amorphous Ni_xTi_{1-x} alloys with (R_1, R_{12}, R_2) = (2.40, 2.45, 2.85) Å. As described in the text, the density ρ is assumed, to a first approximation, to be a linear function of the Ni concentration x_1.

x_1	ρ	Z_{11}	Z_{12}	Z_{22}	α_w
0.3	0.062	1.38	7.63	8.74	−0.100
0.5	0.068	3.96	6.86	6.86	−0.118
0.7	0.075	7.36	4.01	3.08	−0.103

$x_1 = 0.3$; with increasing Ni content, the height of the second component of the split peak decreases and the double structure is absent for $x_1 = 0.7$.

In figure 8, as x_1 is varied from 0.3 to 0.7, the position of the first peak of $S^x(k)$ moves towards larger k values. It is interesting that this shift, which corresponds semi-quantitatively to the true experimental behaviour (Moine *et al* 1985), is explained by the model simply in terms of density changes, without varying the diameters R_{ij}. Furthermore, the inset shows that, at least within our approximations, the prepeak tends to become a shoulder with increasing Ni concentration.

Finally, the behaviour of the structural parameters Z_{ij} and α_w with varying compositions is shown in Table 3.

4. Discussion

Before concluding, we wish to comment on the three basic aspects of the present work, i.e., (*a*) the NAHS potential, (*b*) the Percus–Yevick approximation, and (*c*) the use of integral equations. We also discuss the problem of the second peak splitting of the $S^x(k)$.

(*a*) As concerns the NAHS potential, a first point of interest is the comparison between the NAHS model and the symmetric HSY one, which has been the most frequently used for reproducing CSRO in liquid metallic alloys (even for phase-separating mixtures). The convenience of the symmetric HSY model lies in the fact that the relevant conditions of equality of HS diameters and charge neutrality, with the combined use of the mean spherical approximation (MSA), allow a reduction of the three OZ equations to two independent relations. This simplification then enables one to find an analytic solution. It is well known, however, that the aforesaid special symmetry conditions yield to a complete decoupling of the number density and concentration fluctuations, i.e., $S_{NC}(k) = 0$, which for systems with strong CSRO seems to be unrealistic. Note that, on the contrary, the NAHS potential ensures the necessary coupling between density and concentration fluctuations and therefore, in a merely structural study, it could be preferable for its simplicity. It should be mentioned, however, that efficient numerical algorithms have recently been proposed to find MSA solutions also for asymmetric HSY mixtures (Arrieta *et al* 1987, Pastore 1988).

Clearly, the NAHS potential is only a first approximation and more realistic interactions are required to reduce the gap between theory and experiment. As already mentioned, it is reasonable to expect that even a simple softening of the core, for instance a passage to non-additive repulsive inverse-power potentials, could yield

some improvement on our results. Nevertheless, the NAHS model remains of great importance since, used in the context of thermodynamic perturbation theories for more realistic interactions, it can also serve as a better reference system than an additive HS mixture (Kahl and Hafner 1985, 1987).

Both NAHS and HSY potentials could be considered as convenient reference systems to investigate CSRO effects in non-ideal alloys. The explicit presence of long-range interactions in the HSY case should not by itself be taken as an indication of a better modelling of the full Hamiltonian. The similarity of structural results obtained from HSY and NAHS in these systems indicates that the relevant information about CSRO is already contained in the sizes of the repulsive regions. This result supports the point of view, well established in the case of simple one-component liquids, that the main structural properties are fixed by the repulsive part of the potential, while thermodynamics needs a more detailed treatment of the interaction and the inclusion of the attractive part. Then, if we are interested in the structural properties only, the NAHS has the advantage of reducing the number of free parameters to the minimum.

(*b*) Our choice of the PY approximation was motivated by its simplicity and the success of its predictions for HS systems in the fluid phase. Moreover, for a first approximation model a high accuracy was unnecessary and, consequently, we were not excessively worried about the shortcomings of the PY closure. For instance, it is well known that, at high packing fractions, the first minimum of the PY $g_{ij}(r)$ may sometimes go negative. In practice, we found that the introduction of negative non-additivity often reduces or eliminates this unphysical feature, probably because of the consequent lowering of the packing fraction (in our best result for the $Ni_{40}Ti_{60}$ alloy the first minima in the RDFs are very low but positive).

However, one could always try to overcome, at least partly, this and other failures of the PY approximation, by using a different closure for the OZ integral equations. Here we would mention only the thermodynamically self-consistent Rogers–Young closure, recently applied to a 'soft-sphere' model for glass-forming alloys (Bernu *et al* 1987), as well as the less known but efficient Martynov–Sarkisov approximation, already used also for NAHS mixtures (Ballone *et al* 1986).

(*c*) Finally, the validity of extending an integral equation approach of the equilibrium theory of liquids to the study of amorphous solid materials should be discussed. To this end, it would be instructive to compare our results with those obtained by different statistical mechanical routes, in particular by computer simulation methods (i.e., dense random packing algorithms, Monte Carlo procedures and molecular dynamics, MD) that have been employed successfully in structural investigations into mono- and multi-component amorphous systems.

A comparison with dense random packed models is, however, difficult, since they often involve additional potential terms required for energy relaxations and their results may be strongly dependent on details of the packing algorithm, as recently shown for the CSRO parameter α_w (Saw and Faber 1985, Saw and Schwarz 1985).

On the other hand, we are aware of very few MD studies concerning specifically CSRO in binary alloys and using the Bhatia–Thornton formalism (for instance, the work by Jacucci *et al* (1985) on liquid Li_4Pb and by Hafner and Pasturel (1985) on liquid and amorphous $Mg_{70}Zn_{30}$). However, computer simulation 'experiments' have been performed extensively to study the metallic liquid–glass transition and the relevant results may be useful also to discuss the problem of the absence of a second peak splitting in our theoretical $S^x(k)$.

As is well known, the experimentally evident presence of splittings or even shoulders in the second peak of the $g_{ij}(r)$ and $S^x(k)$ has often been taken as a 'signature'

of the glassy state (Dixmier and Sadoc 1978), although there is no clear way to relate such features of static structural properties to the dynamic and thermodynamic behaviour, which only allow a meaningful distinction between a liquid and an amorphous solid. Now, it is to be noted that, when one compares these second peak substructures of the experimental RDFs with computer simulation and integral equation results, it is often evident that the integral equations systematically underestimate the phenomenon and sometimes do not reproduce the RDF splitting obtained, on the contrary, in the computer calculations.

Unfortunately, the reason for such a discrepancy between integral equation approach and computer simulations is not completely clear and, at present, we can only suggest two possible causes. First, the existing closures for the OZ equations can be seen as originated from different approximations to the higher-order, many-body, correlation functions in terms of pair correlations. These approximations might give a good description of the region around the first RDF peak (more important for $S^x(k)$ and the thermodynamic properties), but they can fail in the second peak region, where, in the case of two close second-neighbour shells, the effect of the three-body correlations is expected to be important. Second, according to a viewpoint expressed by other authors (Weeks 1977, Zerah and Hansen 1986, Bernu *et al* 1987, Kambayashi and Hiwatari 1988), the integral equations of the liquid state theory, assuming homogeneity and equilibrium of the system, presumably describe a hypothetical fully relaxed disordered structure, realised by an infinitely slow quenching of the liquid. Consequently, the RDF predictions from integral equations may be different from those obtained by computer simulations of rapid quenching, which can produce true, non-equilibrium glassy states.

At this point we stress, however, that one should separate the analysis of the shape of the $g_{ij}(r)$ from that of the $S^x(k)$ [or $S_{ij}(k)$]. In fact, since the Fourier transform is a non-local mapping of the real space into the reciprocal space, it is not obvious that the second peak splitting in the RDFs should be related to a similar one in $S^x(k)$ or $S_{ij}(k)$ [compare, for instance, figure 5 (8) and figure 14 (15) of Weeks' (1977) paper, as well as figures 5 and 6 of Dixmier and Sadoc (1978)].

While RDF splittings have been analysed extensively (mainly for mono-atomic amorphous systems), to our knowledge a complete understanding of the second peak splitting in the experimental $S^x(k)$ is lacking and we could only try to interpret it as an 'interference' effect, coming out from the onset of a competition between two (or more) frequently repeated distances in real space (Hajdu 1980). In addition, the localisation of the effect at intermediate k values suggests the possibility that it could be due to some feature of the potential at small separations. If this would be the case, it would explain the absence of k-space splitting in our simplified HS model for the interaction.

However, at present we are not able to exclude a discrepancy between computer simulation and integral equation results in this region of the k-space, like in the case of the $g_{ij}(r)$. We believe that the question certainly deserves further investigation and a check of this point is presently under study.

5. Conclusions

First of all, we have demonstrated that a two-component hard-sphere model with negatively non-additive diameters can really reproduce the CSRO present in amorphous

(and liquid) binary mixtures with preferred hetero-coordination. In other words, the concentration fluctuations visible from the Bathia–Thornton structure factor $S_{CC}(k)$ and the consequent pre-peak present in the experimental $S^x(k)$ of Ni–Ti glasses can be explained entirely in geometrical terms (i.e., excluded volume effects), if a partial overlapping of unlike spheres is allowed. According to our model, a less pronounced CSRO is already present in the liquid phase and gradually develops in magnitude with increasing density. Very accurate diffraction studies on the onset of the prepeak as a function of the temperature could verify this point.

We emphasise that the NAHS potential is proposed as a simple satisfactory model for the structure, but not for the thermodynamics, of alloys with weak or strong CSRO. An HS model for the structure is clearly less ambitious than any theory based on some modelling of the full interatomic interaction, but this limit of the model is, paradoxically, one of its more appealing features. The possibility of having a reasonable description of the structure, depending only on a limited set of parameters, allows an approximate decoupling between the problem of the structure and that of the thermodynamics. The usefulness of such a separation is clear when one realizes how difficult is a realistic and reliable determination of an interatomic potential for non-simple metals.

Another point to note is that, to our knowledge, this paper offers the first example of numerical solution of the OZ integral equations for *asymmetric* NAHS systems with *realistic* parameter values for an *amorphous* solid. This means also that the possibility of using NAHS mixtures as a reference system in thermodynamic perturbation theories for more complex potentials is becoming more and more feasible. At present, some simple steps in this direction could already be allowed by the available numerical algorithms, even if general and complete analytic solutions for NAHS models are lacking.

Finally, we have shown that an integral equation approach, which comes out from the liquid state theory and is less time-consuming than computer simulations, can reasonably be applied to amorphous systems, since it yields results in satisfactory overall agreement with the experimental data of Ni–Ti glasses. Even if one assumes that the integral equations describe an ideal 'extrapolation' of the stable fluid structure to higher densities, their results are instructive and should be considered as an indication of how the structure of an amorphous solid is similar to that of the supercooled liquid.

In particular, we have also discussed the second peak splitting in the structure factors and work is in progress to investigate more deeply this interesting feature of amorphous materials.

Acknowledgments

We would like to thank Professor T Fukunaga for sending us numerical tables of experimental structure factors for the $Ni_{40}Ti_{60}$ glass.

References

Abernethy G M and Gillan M J 1980 *Mol. Phys.* **39** 839
Arrieta E, Jedrzejek C and Marsh K N 1987 *J. Chem. Phys.* **86** 3607

Ashcroft N W and Langreth D C 1967 *Phys. Rev.* **156** 685
Ballone P, Pastore G, Galli G and Gazzillo D 1986 *Mol. Phys.* **59** 275
Bernu B, Hansen J P, Hiwatari Y and Pastore G 1987 *Phys. Rev.* **A36** 4891
Bhatia A B and Thornton D E 1970 *Phys. Rev.* B **2** 3004
Boublik T, Nezbeda I and Hlavaty K 1980 *Statistical Thermodynamics of Simple Liquids and Their Mixtures* (Amsterdam: Elsevier)
Cargill G S III 1975 *Solid State Phys.* **30** 227 (New York: Academic)
Copestake A P, Evans R, Ruppersberg H and Schirmacher W 1983 *J. Phys. F: Met. Phys.* **13** 1993
Dixmier J and Sadoc J F 1978 *Metallic Glasses* ed. J J Gilman and H J Leamy (Ohio: Am. Soc. Metals) ch 4
Enzo S, Schiffini L, Battezzati L and Cocco G 1988 *J. Less-Common Met.* **140** 129
Fukunaga T, Kai K, Naka M, Watanabe N and Suzuki K 1981 *Proc. 4th Int. Conf. Rapidly Quenched Metals*, vol 1 ed. T Masumoto and K Suzuki (Sendai: Japan Institute of Metals) p 347
Fukunaga T, Watanabe N and Suzuki K 1984 *J. Non-Cryst. Solids* **61/62** 343
Gazzillo D 1987 *J. Chem. Phys.* **87** 1757
—— 1988 *Mol. Phys.* **64** 535
Gillan M J 1979 *Mol. Phys.* **38** 1781
Greenwood D A 1980 *J. Phys. C: Solid State Phys.* **13** 331
Hafner J 1977 *Phys. Rev.* A **16** 351
—— 1980 *Phys. Rev.* B **21** 406
—— 1985 *Amorphous Solids and the Liquid State* ed. N H Marsh, R A Street and M P Tosi (New York: Plenum) ch 4
Hafner J and Kahl G 1984 *J. Phys. F: Met. Phys.* **14** 2259
Hafner J and Pasturel A 1985 *J. Physique Coll.* **46** C8–367
Hafner J, Pasturel A and Hicter P 1984 *J. Phys. F: Met. Phys.* **14** 1137
Hajdu F 1980 *Phys. Status Solidi* a **61** 141
Hansen J P and Schiff D 1973 *Mol. Phys.* **25** 1281
International Tables for X-ray Crystallography 1969 vol 4 (Birmingham: Kynoch) p 71
Jacucci G, Ronchetti M and Schirmacher W 1985 *J. Physique Coll.* **46** C8–385
Kahl G and Hafner J 1985 *J. Phys. F: Met. Phys.* **15** 1627
—— 1987 *Phys. Chem. Liquids* **17** 139
Kambayashi S and Hiwatari Y 1988 *Phys. Rev.* A **37** 852
Kittel C 1976 *Introduction to Solid State Physics* 5th edn (New York: Wiley)
Lebowitz J L and Zomick D 1971 *J. Chem. Phys.* **54** 3335
Lele S 1984 *Metallic Glasses. Production, Properties and Applications* ed. T R Anantharaman *Materials Science Surveys No 2* (Switzerland: Trans Tech Publications)
Levesque D, Nixon J H, Silbert M and Weis J J 1980 *J. Physique Coll.* **41** C8–317
Moine P, Naudon A, Kim J J, Marshall A F and Stevenson D A 1985 *J. Physique Coll.* **46** C8–223
Nixon J H and Silbert M 1984 *Mol. Phys.* **52** 207
Pastore G 1988 *Mol. Phys.* **63** 731
Pasturel A, Hafner J and Hicter P 1985 *Phys. Rev. B* **32** 5009
Perry B N and Silbert M 1979 *Mol. Phys.* **37** 1823
Polk D E, Calka A and Giessen B C 1978 *Acta Metall.* **26** 1097
Ruppersberg H and Hegger H 1975 *J. Chem. Phys.* **63** 4095
Ruppersberg H, Lee D and Wagner C N J 1980 *J. Phys. F: Met. Phys.* **10** 1645
Sakata M, Cowlam N and Davies H A 1981 *J. Phys. F: Met. Phys.* **11** L157
Saw C K and Faber J Jr 1985 *J. Non-Cryst. Solids* **75** 347
Saw C K and Schwarz R B 1985 *J. Non-Cryst. Solids* **75** 355
Schwarz R B, Petrich R R and Saw C K 1985 *J. Non-Cryst. Solids* **76** 281
Wagner C N J and Lee D 1980 *J. Physique Coll.* **41** C8–242
Wagner C N J, Lee D, Keller L, Tanner L E and Ruppersberg H 1981 *Proc. 4th Int. Conf. Rapidly Quenched Metals* vol 1, ed. T Masumoto and K Suzuki (Sendai: Japan Institute of Metals) p 331
Waseda Y 1984 *Springer Lecture Notes in Physics* vol 204 (Berlin: Springer) ch 2
Weeks J D 1977 *Phil. Mag.* **35** 1345
Zerah G and Hansen J P 1986 *J. Chem. Phys.* **84** 2336